



**HAL**  
open science

# Changes in the distribution of cold waves in France in the middle and end of the 21st century with IPSL-CM5 and CNRM-CM5 models

Sylvie Parey, Thi Thu Huong Hoang

► **To cite this version:**

Sylvie Parey, Thi Thu Huong Hoang. Changes in the distribution of cold waves in France in the middle and end of the 21st century with IPSL-CM5 and CNRM-CM5 models. *Climate Dynamics*, 2015, 47 (3-4), pp.879-893. 10.1007/s00382-015-2877-6 . hal-01569003

**HAL Id: hal-01569003**

**<https://hal.science/hal-01569003>**

Submitted on 26 Jul 2017

**HAL** is a multi-disciplinary open access archive for the deposit and dissemination of scientific research documents, whether they are published or not. The documents may come from teaching and research institutions in France or abroad, or from public or private research centers.

L'archive ouverte pluridisciplinaire **HAL**, est destinée au dépôt et à la diffusion de documents scientifiques de niveau recherche, publiés ou non, émanant des établissements d'enseignement et de recherche français ou étrangers, des laboratoires publics ou privés.

# Changes in the distribution of cold waves in France in the middle and end of the 21st century with IPSL-CM5 and CNRM-CM5 models

S. Parey, T.T.H. Hoang

EDF/R&D 6, quai Watier 78 401 Chatou Cedex France

Tel : 33 1 30 87 76 14

Fax : 33 1 30 87 71 08

[sylvie.parey@edf.fr](mailto:sylvie.parey@edf.fr)

**Abstract:** In this paper, a stochastic model is used to simulate daily minimum temperature time series coming from observations and two CMIP5 climate models (IPSL-CM5A-MR and CNRM-CM5) in order to analyze the changes in cold wave number and proportions under future climate conditions. The stochastic model allows computing 100 temperature time series for each different source (observation or climate model), and for 22 locations in France, which enables inferring the statistical significance of the changes. Two future time periods, near (around 2010 to 2060) and far future (around 2050 to 2100), and two RCPs (RCP4.5 and RCP8.5) are considered, while 3 different thresholds are used to identify cold waves: 0°C and the 10<sup>th</sup> and 5<sup>th</sup> percentiles of observed wintertime (December-January-February) daily minimum temperature distribution. The results show that both models project a significantly lower number of cold waves in the future, all durations considered, but the changes mainly concern the proportion of the longest cold waves (10 days and more). The decreases are higher with IPSL-CM5A-MR than with CNRM-CM5. The main driver of this change is the decreasing frequency of the observation based thresholds in the future, which is higher for IPSL-CM5-MR model because the impact of a higher mean is enhanced by a decrease in the variance.

*Keywords: Climate change; cold waves; stochastic modelling*

## 1. Introduction

In the climate change context, more and more studies are devoted to the evolution of extreme events, since those have a major impact on people, society and organizations. Among these events, temperature related ones, heat and cold waves, are of special concern for electricity companies, because they impact both electricity production and demand. Agriculture, road or rail management or health are other examples of impacted sectors. In 2012, IPCC devoted a special report to the assessment of this issue of climate change and extreme events: the Special Report on Managing the Risks of Extreme Events and Disasters to Advance Climate Change Adaptation (SREX). Its main conclusions about temperature related extremes were that “it is very likely that there has been an overall decrease in the number of cold days and nights, and an overall increase in the number of warm days and nights, on the global scale” and “it is virtually certain that hot extremes will increase and cold extremes will decrease over

38 the 21<sup>st</sup> century with respect to the 1960-1990 climate”. However, the same report also noted  
39 that fewer studies had been devoted to the analysis of cold or warm spells compared to those  
40 devoted to changes in the frequency and intensity of cold or warm days and nights. As a  
41 consequence, less robust conclusions could have been given for those events, and essentially  
42 concern warm events: “There is medium confidence that the length or number of warm spells,  
43 including heat waves, has increased since the middle of the 20<sup>th</sup> century”. Nevertheless, the  
44 report stated that “it is very likely that the length, frequency and/or intensity of warm spells,  
45 including heat waves (defined with respect to present day climate) will increase over most  
46 land areas.” Then, IPCC AR5 working group I report further supported those conclusions, in  
47 more strongly assessing the anthropogenic contribution to the observed changes. Furrer et al.  
48 (2010) and Wang et al. (2014) also have investigated the hot spell behavior by using extreme  
49 value theory. Cold waves are however an important issue for electricity management,  
50 especially in France where electrical heating is important.

51 In a recent set of papers, Sillmann et al. (2013) applied the climate extreme indices defined by  
52 the Expert Team on Climate Change Detection and Indices (ETCCDI) to a large number of  
53 CMIP5 and CMIP3 simulations (Coupled Model Intercomparison Projects phases 5 and 3).  
54 Among these indices, CSDI represents cold spell duration, and their results show that CMIP5  
55 models agree with ERA-40 and ERA-Interim re-analyses in representing a decreasing trend in  
56 the cold spell duration over the period 1948-2005. Part 1 is dedicated to model evaluation,  
57 then, in part 2, they found significant changes in CSDI over land in the end of the 21<sup>st</sup> century,  
58 with around 3.4 days less according to a RCP2.6 scenario, 3.9 days less for RCP4.5 and 4.2  
59 days less for RCP8.5, the changes being coherent but weaker for CMIP3 models. At the  
60 European scale, De Vries et al. (2012) studied western European cold spells (where  
61 temperature falls below the 10<sup>th</sup> percentile of the winter daily mean temperature distribution)  
62 in current and future climate. They showed that most of the changes in cold spell statistics can  
63 be explained by changes in mean (increase) and variance (decrease) of the winter temperature  
64 distribution. This dominating role of the evolutions of mean and especially variance in the  
65 evolutions of temperature extremes had also been found by Parey et al (2010). Concerning  
66 France, Cattiaux et al. (2013a) first studied the link between hot and cold spells and the  
67 dynamic circulation and its reproduction by different versions and resolutions of the IPSL  
68 climate model. They found that the model version used for CMIP5 tends to improve the  
69 wintertime dynamics and the statistics of cold spells. In another paper, Cattiaux et al. (2013b)  
70 focused on changes in cold extremes over Europe in a pilot study using both French climate  
71 models (IPSL and CNRM) AMIP (Atmospheric Model Intercomparison Project) experiments.

72 Large decreases in the number of extremely cold days at the end in the 21<sup>st</sup> century are  
73 reported, mainly driven by non dynamical mechanisms. Peings et al. (2012) analyzed the  
74 representation of observed cold waves and their change at the end of the 21<sup>st</sup> century  
75 according to a RCP8.5 scenario with 13 CMIP5 models. They found that model biases mostly  
76 concern intensity rather than geographical extent and duration, and that these events will be  
77 less frequent at the end of the century, except for one model.

78 The present study aims at complementing these results by adopting a different point of view.  
79 We focus here on the local distributions of cold spells of different durations, from one single  
80 day to more than 15 consecutive days below a defined threshold. It is based on a set of high  
81 quality temperature time series provided by Météo-France and on the results of the French  
82 IPSL-CM5A-MR and CNRM-CM5 climate models run in the framework of CMIP5. Note  
83 that the version of IPSL model is different from that used in Peings et al (2012), who used the  
84 results of IPSL-CM5A-LR. Three different thresholds (one fixed, 0°C, and two percentile  
85 based, the 10<sup>th</sup> and 5<sup>th</sup> percentiles of the observed wintertime –December-January-February-  
86 temperature distribution), two future periods (around 2010 to 2060 and the end of the 21<sup>st</sup>  
87 century) and two climate change scenarios (RCP4.5 and RCP8.5) will be considered. The  
88 originality lies in the use of a stochastic model of temperature to bias correct and downscale  
89 the climate change simulations. Climate models are namely designed to faithfully simulate  
90 large scale features of the climate system and its circulations, as well as the main  
91 characteristics of the physical interactions, cycles and their possible evolutions under external  
92 forcing. However, they cannot precisely represent local weather and different downscaling  
93 techniques have been proposed in the literature to overcome this issue for impact studies (see  
94 Maraun et al. 2010 for a review). These techniques can be divided into statistical and  
95 dynamical approaches. Statistical methods are based on some identification of statistical  
96 relationships between large scale and local scale variables used to derive local information  
97 from the larger scale patterns given by the climate model. Dynamical methods consist in  
98 running a limited area climate model forced by the larger scale model at its boundaries in  
99 order to refine the simulation over a chosen small region. The approach used here is a  
100 statistical downscaling technique based on the use of a quite sophisticated stochastic model.  
101 This stochastic model allows moreover the simulation of a large number of equivalent  
102 temperature time series then used to evaluate the statistical significance of the obtained  
103 changes in proportions of cold spells of different duration. Furrer et al. (2010) also proposed a  
104 stochastic model, used by Wang et al. (2015) to study hot spell changes in China from CMIP5

105 simulations, but only hot spells are modelled, not the whole temperature time series as is the  
106 case here.

107 The considered time series, model simulations and the methodology will be described in  
108 section 2, and then section 3 will present the validation of the approach over the current  
109 climate period. Section 4 will be devoted to the analysis of the changes in the cold wave  
110 distribution in the near and far future according to RCP4.5 and RCP8.5 scenarios, before  
111 coming to the conclusion and discussion in section 5.

112

## 113 **2. Data, models and methodology**

### 114 **2.1 Observation time series**

115 In the framework of the French IMFREX project devoted to the impact of climate change on  
116 extreme events, Météo France developed a database of daily time series selected for their  
117 homogeneity over the longest possible period after a procedure of trend and metadata analysis  
118 dedicated to the detection of possible changes in the measurement conditions (Gibelin et al.  
119 2014). These so-called SQRs (Série Quotidiennes de Référence, reference daily time series in  
120 French) constitute a robust database of observations over France to study climate change. A  
121 set of 39 of such temperature time series have been provided by Météo-France for this study,  
122 conducted in the framework of the French national research agency supported SECIF project  
123 (dedicated to the development of climate services for the French industries). Among this set  
124 of time series, 22 daily minimum temperature time series have been selected as the longest  
125 and most representative of different locations in France, as shown in Figure 1, and they cover  
126 periods between 1953 and 2011. However, since the historical simulations of the climate  
127 models end in 2005, the observation time series are considered over periods between their  
128 beginning year and 2005. Table 1 summarizes the observed time series periods considered.  
129 The selection aimed at attributing a single station to a climate model grid cell, and thus when  
130 stations are too close, only the longest one is selected.

### 131 **2.2 Climate models**

132 The CNRM-CM5 and IPSL-CM5A-MR coupled ocean atmosphere GCMs are described  
133 respectively in Voltaire et al. (2013) and Dufresne et al. (2012) and will just be briefly  
134 presented here. The atmospheric component of CNRM-CM5 is the spectral ARPEGE-Climat  
135 GCM with a T127 linear grid (256 x 128 grid points) with 31 vertical levels. The ISBA land  
136 surface model, the NEMO ocean model and the GELATO sea ice model are coupled to the  
137 atmospheric model through the AOSIS coupler. The atmospheric component of IPSL-CM5A-

138 MR is the LMDZ model which has a 144x143 regular grid and 39 vertical levels, and is  
139 coupled to the ORCHIDEE land surface scheme. The ocean model is the NEMO-OPA suites,  
140 which models interactions of ocean, sea ice and marine ecosystem. Ocean atmosphere  
141 coupling is done through the OASIS coupler. CNRM-CM5 and IPSL-CM5A-MR models  
142 have different physical parameterizations and only share a closely resembling radiative  
143 scheme.

144 For each model, the historical simulation, covering period 1950-2005, and two scenario runs,  
145 RCP4.5 and RCP8.5, covering period 2006-2100 are considered. For current climate, model  
146 simulations are considered over the exact same period as that of the corresponding  
147 observation time series. For example, for an observation time series spanning the period 1954-  
148 2005, the model historical simulation is considered for years 1954 to 2005. Two future  
149 periods are then considered, one ending in 2060 and the other ending in 2100, the length  
150 being chosen identical to the observation time series length for convenience. Thus, again, for  
151 an observation time series covering 1954-2005, the first future period is 2009-2060 and the  
152 second one 2049-2100.

### 153 **2.3 Stochastic temperature model**

154 As stated before, a stochastic temperature model is used to bias correct and downscale the  
155 temperature time series provided by the climate models. This temperature generator is  
156 designed to realistically reproduce temperature extremes, and potentially simulate larger  
157 extremes than observed. It is a stochastic Functional Seasonal Heteroscedastic Auto  
158 Regressive model used to simulate the stochastic part of the process after the deterministic  
159 parts, trends and seasonalities in the mean and the variance, have been removed. It has namely  
160 been found from analyses of a large number of different temperature time series that once  
161 trends and seasonalities in the mean and the variance have been removed, no trends can be  
162 identified in the other moments (up to moment 4), the auto-correlations and in the extremes of  
163 the residuals (Hoang 2010). However, some seasonality remains in the other moments and in  
164 the auto-correlations, but not really in the extremes. Thus the stochastic model simulates  $Z(t)$ ,

165 where

$$Z(t) = \frac{X(t) - S_m(t) - m(t)}{S_v(t)s(t)} \quad (1)$$

166 with  $X(t)$  the observed temperature time series,  $S_m(t)$  the seasonality of the mean,  $m(t)$  the  
167 trend in mean,  $S_v(t)$  the seasonality of the standard deviation, and  $s(t)$  the trend in standard  
168 deviation. This corresponds to a standardization based on two deterministic parts of mean and  
169 standard deviation (seasonality and trend) rather than on their constant value estimated over

170 the whole time period. The seasonalities are identified as trigonometric polynomials of the  
 171 form

$$172 \quad \theta_0 + \sum_{i=1}^p (\theta_{i,1} \cos \frac{2i\pi t}{365} + \theta_{i,2} \sin \frac{2i\pi t}{365}) \quad (2)$$

173 where the order  $p$  is chosen according to an Akaike criterion. The non parametric trends are  
 174 estimated by LOESS with an optimal smoothing parameter obtained through a modified  
 175 partitioned cross-validation technique (Hoang 2010; Dacunha-Castelle et al. 2015; Parey et al.  
 176 2014). Then,  $Z(t)$  is modeled as:

$$177 \quad Z(t) = b(t)Z(t-1) + a(t, Z(t-1))\varepsilon_t \quad (3)$$

178 With

$$179 \quad b(t) = \theta_0 + \sum_{j=1}^{p_1} (\theta_{j,1} \cos \frac{2j\pi t}{365} + \theta_{j,2} \sin \frac{2j\pi t}{365}) \quad (4)$$

180  $p_1$  being again chosen according to an Akaike criterion, and  $a$  is the conditional standard  
 181 deviation, obtained from the conditional variance  $a^2$  estimated as:

$$182 \quad a^2(t, Z(t-1)) = (\hat{r}_2 - t)(t - \hat{r}_1) \sum_{k=0}^5 \sum_{j=1}^{p_2} (\alpha_{1,k}^j \cos \frac{2j\pi t}{365} + \alpha_{2,k}^j \sin \frac{2j\pi t}{365}) Z(t-1)^k \quad (5)$$

183 under constraints for its first derivatives at the boundaries:

$$184 \quad (a^2)'(r_1) = \frac{2b(r_1)}{1 - \frac{1}{\xi_1}} \quad \text{and} \quad (a^2)'(r_2) = \frac{2b(r_2)}{1 - \frac{1}{\xi_2}}, \quad a^2(t, Z(t-1)) > 0 \forall t$$

$$185 \quad (6)$$

186 and  $p_2$  chosen by Akaike criterion. Extreme value distributions for temperature are known as  
 187 bounded, thus the simulation of the residuals  $Z(t)$  has to support this behavior and  $Z(t)$  is  
 188 defined over an interval  $[r_1, r_2]$ .  $r_1$  and  $r_2$  correspond to the estimated bounds of the extreme  
 189 value distributions for the left and right tails of  $Z(t)$ . The constraints for the derivatives of the  
 190 conditional variance are meant to force it to reach zero at the boundaries. The details and  
 191 mathematical justifications for these choices can be found in Dacunha-Castelle et al. (2015).

192 The bounds  $r_1$  and  $r_2$  are estimated by application of the extreme value theory to the  $Z(t)$  time-  
 193 series obtained from the observations, and  $\xi_1$  and  $\xi_2$  are the shape parameters estimated for the  
 194 lower and upper tail by fitting a Generalized Extreme Value distribution to the block maxima  
 195 (as the extremes of  $Z(t)$  are stationary, a block length of 73 days is used in order to select a  
 196 sufficient number of maxima to more reliably fit the distribution).  $\varepsilon_t$  is the random part and is  
 197 defined as a truncated normal distribution whose truncation depends on the value of  $Z(t-1)$ .

198 Then a simulation of the initial temperature time series is obtained by re-introducing the  
199 estimated deterministic parts.

200 The stochastic model is fitted to the residuals obtained from the observed time series, and  
201 then, seasonalities and trends coming either from the observations or from the climate model  
202 time series are used to reconstruct temperature time-series from the simulated residual time  
203 series. In this study, 100 simulations of the residuals for each of the 22 observed temperature  
204 time series have been considered.

## 205 **2.4 Simulated temperature time series**

206 As stated before, for each location 100 time series of the residuals  $Z(t)$ , after removing trends  
207 and seasonalities, are computed. The ability of the model to reproduce the observed behavior  
208 of  $Z(t)$  has been checked in Hoang (2010), Dacunha-Castelle et al. (2015) and Parey et al.  
209 (2014), thus, from these, 100 temperature time series coherent with the observed one are  
210 obtained by reintroducing trends and seasonalities. For climate model temperature time series,  
211 potential biases have first to be investigated. Seasonality is the first estimated deterministic  
212 part, and trend is identified from the time series of anomalies from the seasonality. The same  
213 procedure is applied to observed and model temperature time series, and when comparing the  
214 obtained seasonalities and trends, it appears that most of the model bias is embedded in the  
215 seasonality identification, while trends are then more coherent with the observed ones. Figure  
216 2 illustrates this point for the station of Cannes, in the south of France. Thus, the reconstructed  
217 temperature time series for present climate are built by adding (multiplying by for standard  
218 deviation) observed seasonalities and climate model trends to the simulated residuals  $Z(t)$ .  
219 Then, for future time periods, seasonalities are obtained by adding the modeled difference in  
220 seasonality of the mean between future and present period for the seasonality in the mean, and  
221 multiplying by the ratio of future period standard deviation seasonality to present period one  
222 for the seasonality of the standard deviation:

223  $S_{mf} = S_{mo} + (S_{mm2} - S_{mm1}); \quad S_{vf} = S_{vo} * S_{vm2}/S_{vm1}$  with  $S_m$  denoting seasonality of the  
224 mean,  $S_v$  seasonality of the standard deviation, and subscripts f, o, m1 and m2 denoting  
225 respectively future period, observation, model present period and model future period. Figure  
226 3 illustrates such a reconstruction for the same station of Cannes.

## 227 **2.5 Cold waves**

228 Cold waves are defined here as cold spells with one or more consecutive days with daily  
229 minimum temperature below a chosen low threshold. In this study, three thresholds are  
230 considered: a fix threshold,  $0^\circ\text{C}$ , and two low percentiles: the 10<sup>th</sup> and 5<sup>th</sup> percentiles of the



231 observed wintertime daily minimum temperature distribution over the observation period.  
232 Winter is the climatological winter covering the months of December, January and February  
233 (DJF).

234

### 235 **3. Validation for present period**

#### 236 **3.1 Climate and stochastic models performances**

237 In a first step, the repartitions of all identified cold spells for each station between different  
238 durations are compared for observation and climate model present period simulations. As  
239 climate models have biases, the thresholds used to define cold waves are chosen as the  
240 corresponding percentiles of the climate model time series. Thus, the fixed 0°C threshold is  
241 not 0°C for the models, but the value corresponding in the model time series to the percentile  
242 of 0°C in the observations. The 5<sup>th</sup> and 10<sup>th</sup> percentile of wintertime temperature correspond  
243 similarly to different temperature values in the model runs and in the observations. The  
244 comparisons show that generally, both climate models tend to produce fewer 1-day events and  
245 more 2 days and more ones than observed, and may have difficulties to reproduce very long  
246 cold spells. The stochastic model generally leads to a better reproduction of the proportion of  
247 long events, but tends to overestimate that of 1-day ones. Figure 4 illustrates this behavior for  
248 the station of Tomblaine and the 10<sup>th</sup> percentile threshold. It can be noticed that the stochastic  
249 model is able to produce long cold waves in some simulations, even though none has been  
250 observed (14 days or >15 days in Figure 4 right panel). With a more extreme threshold like  
251 the 5<sup>th</sup> percentile of wintertime temperature, the climate and stochastic models both have  
252 difficulties to produce a similar proportion of very long events as observed, although the  
253 stochastic model again sometimes succeeds in producing some among the 100 simulations,  
254 even though none have been observed.

255 Besides, using the stochastic model allows inferring significance for the observed changes  
256 with the computation of the 95% confidence interval for the distributions obtained from the  
257 100 simulations of each proportion of cold spell duration. Figure 5 illustrates the mean  
258 number of cold waves per year for the 0°C threshold, all durations gathered, for the different  
259 considered locations in France. Black circles indicate the stations for which the simulated  
260 mean number is significantly different from the observed one (the observed number does not  
261 fall inside the 95% confidence interval of simulated numbers). These discrepancies are mainly  
262 due to the previously mentioned tendency to produce much more 1-day events than observed,  
263 whereas the proportions of longer cold spells are more faithfully represented. Then, the

264 repartitions of cold spells computed from the stochastic simulations for the current period  
265 reconstructed with observed seasonalities and trends or observed seasonalities and climate  
266 model trends are very similar, as can be seen in Figure 6 for Tomblaine and the longest cold  
267 spells.

### 268 **3.2 Use in the climate change context**

269 In order to check the ability of the suggested methodology to be used in the climate change  
270 context, a cross-validation has been conducted for one location. The temperature time series  
271 of Champhol, observed over period 1954 and 2005, has been split into two periods of equal  
272 length: 1954-1979 and 1980-2005 (26 years each). The stochastic model has been calibrated  
273 over the first period, and 100 simulations have been made. Then, the minimum temperature  
274 time series for the second period has been reconstructed using first period seasonalities  
275 corrected using climate model seasonality differences between both periods and climate  
276 model trends for the second period, following the suggested methodology for future climate.  
277 Figure 7 shows that the obtained proportions of cold spells are similar to that which would  
278 have been obtained by using observed period 2 seasonalities and trends. Figure 7 is for the  
279 10<sup>th</sup> percentile threshold but this holds true for all used thresholds. This result gives  
280 confidence in the use of this methodology to derive bias corrected future temperature time  
281 series.

282

## 283 **4. Future changes in cold waves number and repartitions**

284

### 285 **4.1 Cold waves number**

286 Then, the changes projected for the future are analyzed, considering the same observation  
287 based thresholds for the present and future periods. In line with all previous studies on the  
288 subject, the mean number of cold spells per year, all durations considered, decreases  
289 whichever the future time period, RCP scenario or threshold chosen for the identification. For  
290 the nearest future period until 2060, both scenarios not surprisingly give relatively similar  
291 results for both models, but IPSL-CM5A-MR model generally projects larger decreases than  
292 CNRM-CM5: around 1 to 5 less episodes per year for 0°C, up to 2 less for the 5<sup>th</sup> percentile  
293 and around 2 to 3 less for the 10<sup>th</sup> percentile with IPSL-CM5A-MR and around 1 to 4 less  
294 episodes per year for 0°C, 1 (more rarely 2) less for the 5<sup>th</sup> percentile and 1 to 2 less for the  
295 10<sup>th</sup> percentile with CNRM-CM5. The decreases are larger for the far future period with  
296 generally one to 2 events less than for the nearest period. Figure 8 illustrates these results for

297 the 10<sup>th</sup> percentile threshold and each model and both near and far future periods for RCP4.5.  
298 The black circles denote significant changes and show that all changes are significant.

299

#### 300 **4.2 Cold waves repartitions**

301 We just saw that the mean number of excursions under the different thresholds, whatever their  
302 lengths, is projected to decrease in the future. Now, let's go further and see how the  
303 repartition among the different event durations is changed. Among this lower total number of  
304 cold spells, in the nearest future period, only the proportion of the longest events (15 days and  
305 more for 0°C, 10 days and more for the 5<sup>th</sup> percentile and 11 to 12 days or more for the 10<sup>th</sup>  
306 percentile) significantly decreases, and once again, more according to IPSL-CM5A-MR  
307 model than according to CNRM-CM5 model. The results are again similar for both RCPs  
308 until 2060, although a little bit higher for RCP8.5. For the end of the century, the picture looks  
309 similar but the significant decreases concern all stations and begin for shorter events. Here,  
310 the impact is larger with RCP8.5 than with RCP4.5, IPSL-CM5A-MR giving again a stronger  
311 response than CNRM-CM5. Significant decreases in proportions concern events during 5  
312 days and more for 0°C, 8 days or more (4 days at some locations) for the 5<sup>th</sup> percentile and 10  
313 days or more (again, less for less cold places) for the 10<sup>th</sup> percentile. Figure 9 illustrates these  
314 results for the period until 2100, both models and scenarios and for the 5<sup>th</sup> percentile  
315 threshold.

316

#### 317 **4.3 Role of observation based threshold in the changes**

318 Previous results are obtained with the same threshold for the identification of cold waves for  
319 present and future periods. However, due to climate change, these thresholds become rarer in  
320 both future periods than nowadays. In order to identify the impact of this change on previous  
321 results, the cold spell repartitions have been estimated again from the stochastic simulations  
322 of the observations, but using as thresholds the values corresponding to the previously defined  
323 threshold location in future wintertime temperature distributions. Thus, the observation based  
324 5<sup>th</sup> and 10<sup>th</sup> threshold for example correspond to 2<sup>nd</sup> to 4<sup>th</sup> and 5<sup>th</sup> to 8<sup>th</sup> percentile for the  
325 nearest period, around 1<sup>st</sup> and 2<sup>nd</sup> to 4<sup>th</sup> percentile for the late period, depending on the model  
326 scenario and location. They thus lie in the farthest tail of the distribution, which could largely  
327 explain the observed changes in number and repartitions of cold waves. When using such  
328 threshold for the observations and comparing to the previously obtained results for the future  
329 periods, we can observe that they generally look very similar, confirming the upmost role  
330 played by this threshold change in the obtained results. Figure 10 illustrates this comparison

331 for the late period (late 2040s to 2100), RCP4.5 and the current period 5<sup>th</sup> percentile of  
332 wintertime temperature distribution as threshold. Significant changes appear for similar cold  
333 spell lengths, the differences rarely exceeding one or 2 days. For one station and IPSL-CM5-  
334 MR, a difference of 4 days can be noticed (circled in red in Figure 9): the significant decrease  
335 is found from 13 days with the observation based threshold and 9 days with the future one.  
336 After checking, it appears that the simulations do not produce 9-day cold spells with the  
337 future threshold, but produce a similar (even slightly higher) proportion of 10-day ones, and  
338 then, for the longest spells, the results are coherent. As the 10-day spells do not change, the  
339 coherent decrease is rather for 11 days and more and then, the results can be considered as  
340 similar. The reason for this absence of 9-day spells will have to be further investigated, but  
341 the proportion become very small for such lengths and a small change, induced by different  
342 trends, can induce such a result. It seems then that the dynamic of cold spells does not change  
343 much in the future, and the frequency of current cold waves decreases because current cold  
344 temperatures become less frequent. Now let us compare the threshold shifts given by each  
345 climate model. As an example, Figure 11 illustrates them for the station of Boulogne sur mer,  
346 in the north of France: for IPSL-CM5-MR, due to both mean increase and variance decrease  
347 (or location and scale of the distribution), the observation based 5<sup>th</sup> percentile of wintertime  
348 temperature distribution (around -5°C for this station), becomes a 0.5<sup>th</sup> percentile in the future.  
349 Such a decrease in the variance is not projected by CNRM-CM5, and the 5<sup>th</sup> percentile of  
350 observation distribution becomes a 1.5<sup>th</sup> percentile of the future wintertime distribution. Both  
351 mean and variance change impact the percentile change, and the difference in variance change  
352 explains why the impact is found higher with IPSL-CM5-MR than with CNRM-CM5. Cold  
353 spell length decreases in the future mainly because the frequency of current thresholds  
354 decreases, and this decrease is linked to both mean and variance changes. It must be recalled  
355 here that when the threshold becomes rarer, the climate and the stochastic models both have  
356 difficulties to produce long cold waves, which could artificially intensify the identified  
357 impact.

358

## 359 **5 Conclusion and discussion**

360 In this study, a stochastic temperature generator has been used to bias correct and downscale  
361 climate simulation results and analyze the future changes in cold waves number and  
362 repartition. Cold waves are defined as consecutive days (from 1 single day to more than 15  
363 days) with daily minimum temperature below different thresholds: 0°C or the 10<sup>th</sup> and 5<sup>th</sup>

364 percentiles of observed wintertime daily minimum temperature distribution. For future period,  
365 two climate model simulations have been considered, one according to RCP8.5 scenario and  
366 the other according to RCP4.5, with only two climate models used in the framework of the  
367 CMIP5 exercise: CNRM-CM5 and IPSL-CM5A-MR. The main outcomes are the following:

- 368 - Using the stochastic model allows both simulating some very long events, even  
369 though none have been observed, and inferring the significance of changes by use  
370 of the confidence intervals derived from 100 simulations for each period
- 371 - In agreement with all previous studies, a significant decrease in the number of cold  
372 spells is found in the future, whichever the future period, model or scenario
- 373 - Among these fewer cold waves, the decreasing essentially concerns the longest  
374 ones, with smaller differences for the nearest future period, whichever the  
375 scenario, and with CNRM-CM5 model
- 376 - The main driver of the changes is the threshold shift: observation based thresholds  
377 are rarer in the future due to climate warming
- 378 - For IPSL-CM5-MR, the variance decrease add to the mean increase to make  
379 current thresholds even rarer in the future, which explains the highest impact found  
380 with this model

381 The fact that in winter, variance decreases when mean increases, has already been evidenced  
382 in Parey et al. 2010. However, the present study shows that two different models may have a  
383 different behavior in this respect, the decrease in temperature variance being much lower for  
384 CNRM-CM5 than for IPSL-CM5A-MR. This study should thus be extended to the  
385 consideration of more climate models. It could be interesting to apply the same methodology  
386 to heat waves too, in order to compare the impacts. Schoetter et al. 2015 also found that for  
387 heat waves, the main driver is the threshold shift, and considering the respective roles of shift  
388 and broadening of the distributions, found no significant change in variance, and thus, a  
389 dominating role for the mean change, whereas here the variance change seems to play a more  
390 important role for cold spells. One advantage of the methodology used here is the  
391 decomposition of the signal between 2 deterministic parts, seasonality and trend, both for  
392 mean and variance, and a stochastic signal. Academic tests will be done with prescribed  
393 changes in the different deterministic components in order to quantify their respective roles in  
394 the change of extreme temperature events. In parallel, suggestions and tests are under way to  
395 improve the stochastic model in order to fix its tendency to produce too much single day  
396 events and too few very long ones, especially when the threshold is extreme (typically lower  
397 than the 5<sup>th</sup> percentile).

398

399 **Acknowledgment:** This work is supported by the SECIF project from the French National Research Agency  
400 (ANR). Special thanks to S. Denvil (IPSL) for providing the CMIP5 simulations, to Paul-Antoine Michelangeli  
401 (EDF/R&D) for preparing and managing the EDF climate model results database, and to G. Gayraud (Météo-  
402 France) for providing the SQR temperature time series.

403

## 404 **6 References**

405 Cattiaux J., Douville H., Ribes A., Chauvin F., Plante C. (2013) : Towards a better  
406 understanding of changes in wintertime cold extremes over Europe: a pilot study with CNRM  
407 and IPSL atmospheric models. *Climate Dynamics*, Volume 40, Issue 9, pp 2433-2445 doi  
408 10.1007/s00382-012-1436-7

409 Cattiaux J., Quesada B., Arakélian A., Codron F., Vautard R., Yiou P. (2013) : North-Atlantic  
410 dynamics and European Temperature Extremes in the IPSL model: sensitivity to atmospheric  
411 resolution. *Climate Dynamics*, Volume 40, Issue 9, pp 2293-2310 doi 10.1007/s00382-012-  
412 1529-3

413 Dacunha-Castelle D., Hoang T.T.H., Parey S. (2015): Modeling of air temperatures:  
414 preprocessing and trends, reduced stationary process, extremes, simulation, *Journal de la*  
415 *Société Française de Statistique*, volume 156, No1, pp 138-168

416 de Vries H, Haarsma RJ, Hazeleger W (2012) Western European cold spells in current and  
417 future climate. *Geophys Res Lett* 39:L04706. doi:10.1029/2011GL050665

418 Dufresne J-L, Foujols M-A, Denvil S., Caubel A., Marti O., Aumont O, Balkanski Y, Bekki  
419 S., Bellenger H, Benshila R, Bony S, Bopp L, Braconnot P, Brockmann P, Cadule P, Cheruy  
420 F, Codron F, Cozic A, Cugnet D, de Noblet N, Duvel J-P, Ethé C, Fairhead L, Fichet T,  
421 Flavoni S, Friedlingstein P, Grandpeix J-Y, Guez L, Guilyardi E, Hauglustaine D, Hourdin F,  
422 Idelkadi A, Ghattas J, Joussaume S, Kageyama M, Krinner G, Labetoulle S, Lahellec A,  
423 Lefebvre M-P, Lefevre F, Levy C, Li Z. X., Lloyd J, Lott F, Madec G, Mancip M, Marchand  
424 M, Masson S, Meurdesoif Y, Mignot J, Musat I, Parouty S, Polcher J, Rio C, Schulz M,  
425 Swingedouw D, Szopa S, Talandier C, Terray P, Viovy N, Vuichard N (2013): Climate  
426 change projections using the IPSL-CM5 Earth System Model: from CMIP3 to CMIP5,  
427 *Climate Dynamics* Volume 40, Issue 9, pp 2123-2165

428 Furrer, E. M., R. W. Katz, M. D. Walter, and R. Furrer (2010): Statistical modeling of hot  
429 spells and heat waves. *Climate Research*, 43, pp 191–205.

430 IPCC (2012): *Managing the Risks of Extreme Events and Disasters to Advance Climate*  
431 *Change Adaptation. A Special Report of Working Groups I and II of the Intergovernmental*

432 Panel on Climate Change, Cambridge University Press, Cambridge, UK, and New York, NY,  
433 USA, 582 pp.

434 IPCC (2013): Climate Change 2013: The Physical Science Basis. Contribution of Working  
435 Group I to the Fifth Assessment Report of the Intergovernmental Panel on Climate Change  
436 [Stocker, T.F., D. Qin, G.-K. Plattner, M. Tignor, S.K. Allen, J. Boschung, A. Nauels, Y. Xia,  
437 V. Bex and P.M. Midgley (eds.)]. Cambridge University Press, Cambridge, United Kingdom  
438 and New York, NY, USA, 1535 pp, doi:10.1017/CBO9781107415324.

439 Gibelin AL, Dubuisson B, Corre L, Deaux N, Jourdain S, Laval L, Piquemal JM, Mestre O,  
440 Denetière D, Desmidt S, Tamburini A (2014): Evolution de la température en France depuis  
441 les années 1950 : Constitution d'un nouveau jeu de séries homogénéisées de référence, La  
442 Météorologie, 87, 45-53, DOI : 10.4267/2042/54336

443 Hoang, T. T. H. (2010), Modélisation de séries chronologiques non stationnaires, non  
444 linéaires: application à la définition des tendances sur la moyenne, la variabilité et les  
445 extrêmes de la température de l'air en Europe, PhD thesis work (written in English),  
446 <http://www.tel.archivesouvertes.fr/tel-00531549/fr/>

447 Maraun D, Wetterhall F, Ireson AM, Chandler RE and others (2010): Precipitation  
448 downscaling under climate change: recent developments to bridge the gap between dynamical  
449 models and the end user. Rev Geophys 48: RG3003, doi: 10.1029/2009RG000314

450 Parey, S., D. Dacunha-Castelle, and T. T. H. Hoang (2010): Mean and variance evolutions of  
451 the hot and cold temperatures in Europe, Climate Dynamics, Volume 34, pp 345–369.

452 Parey, S., T. T. H. Hoang, and D. Dacunha-Castelle (2013): The importance of mean and  
453 variance in predicting changes in temperature extremes, J. Geophys. Res., 118, 8285–8296,  
454 doi:10.1002/jgrd.50629

455 Parey S., Hoang T.T.H., Dacunha-Castelle D. (2014): Validation of a stochastic temperature  
456 generator focusing on extremes and an example of use for climate change, Climate Research,  
457 Vol. 59, pp 61–75

458 Peings Y., Cattiaux J., Douville H. (2013): Evaluation and response of winter cold spells over  
459 western Europe in CMIP5 models. Climate Dynamics, Volume 41, pp 3025-3037, doi  
460 10.1007/s00382-012-1565-z

461 Schoetter R., Cattiaux J., Douville H. (2015): Changes of western European heat wave  
462 characteristics projected by the CMIP5 ensemble. Climate Dynamics, Volume 45, Issue 5, pp  
463 1601-1616

464 Sillmann J., Kharin V.V., Zhang X., Zwiers S.W. and Bronaugh D. (2013): Climate extremes  
465 indices in the CMIP5 multimodel ensemble: Part 1. Model evaluation in the present climate.

466 Journal of Geophysical Research: Atmospheres, volume 118, pp 1716–1733,  
467 doi:10.1002/jgrd.50203

468 Sillmann J., Kharin V.V., Zhang X., Zwiers S.W. and Bronaugh D. (2013): Climate extremes  
469 indices in the CMIP5 multimodel ensemble: Part 2. Future climate projections. Journal of  
470 Geophysical Research: Atmospheres, volume 118, pp 2473–2493, doi:10.1002/jgrd.50188

471 Voldoire A, Sanchez-Gomez E, Salas y Melia D, Decharme B, Cassou C, Senesi S, Valcke S,  
472 Beau I, Alias A et al (2013) The CNRM-CM5.1 global climate model: description and basic  
473 evaluation. Climate Dynamics, Volume 40, Issue 9, pp 2091-2121, doi:10.1007/s00382-011-  
474 1259-y

475 Wang,W., W. Zhou, Y. Li, and X. D. Wang (2014): Statistical modeling and CMIP5  
476 simulations of hot spell changes in China. Climate Dynamics, volume 44, pp 2859-2872.

477

478

479

480

481

482

483

484

485

486

487

488

489

490

491

492

493

494

495

496

497

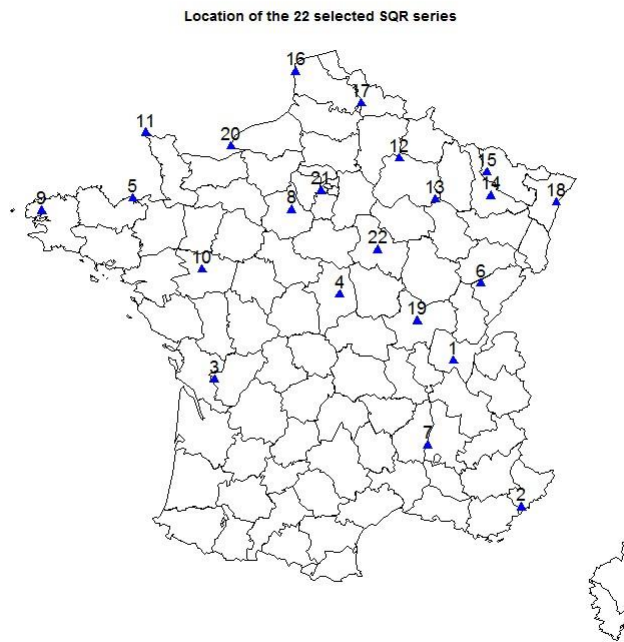
498

499



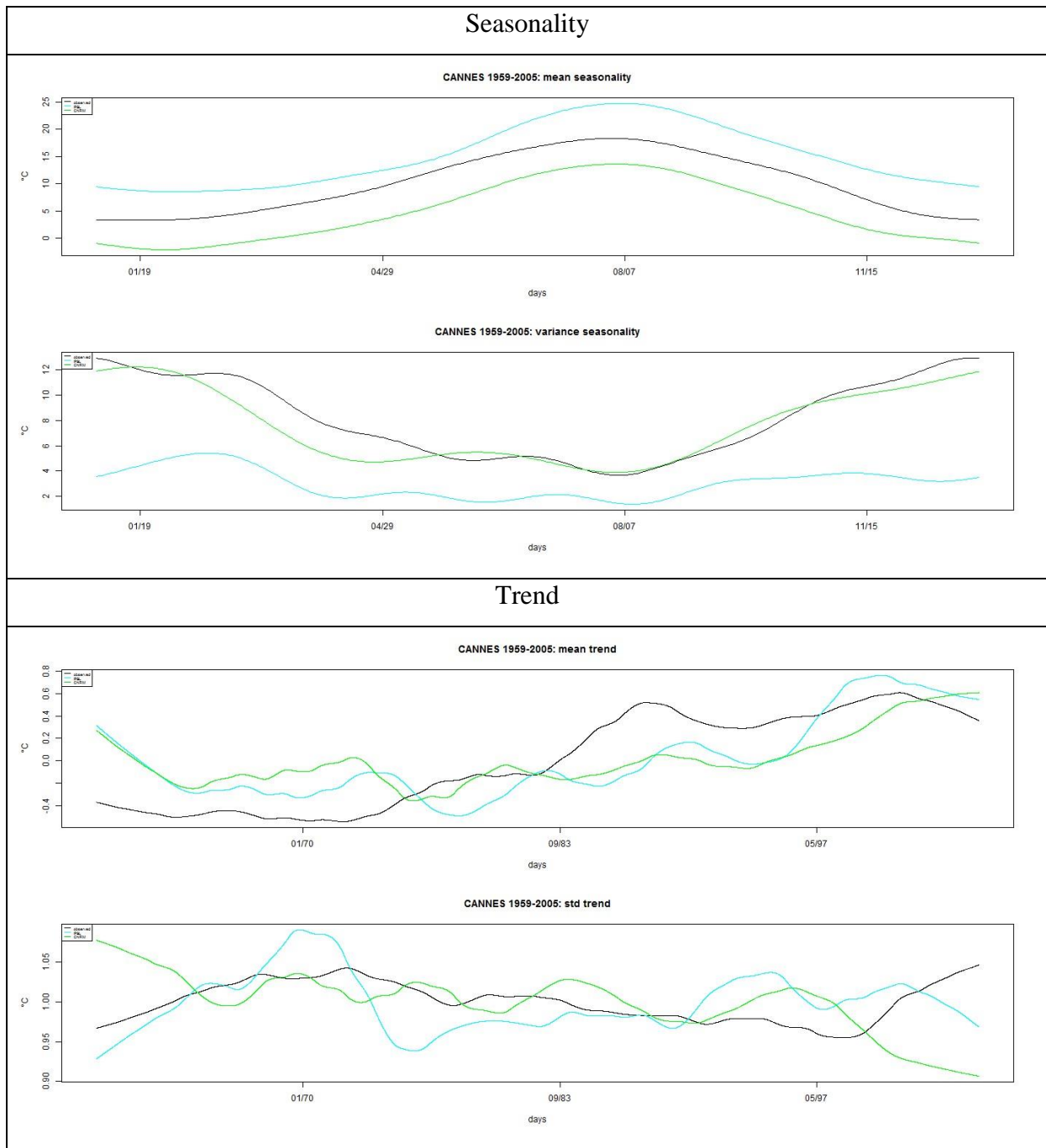
<b>Number</b>	<b>Location</b>	<b>Period</b>
1	Château Gaillard	1953-2005
2	Cannes	1959-2005
3	Chateaubernard	1953-2005
4	Farges en Septaine	1953-2005
5	Saint Cast le Guildo	1955-2005
6	Besançon	1959-2005
7	Montélimar	1959-2005
8	Champol	1954-2005
9	Guipavas	1958-2005
10	Beaucouze	1955-2005
11	Auderville	1955-2005
12	Courcy	1959-2005
13	Saint Dizier	1959-2005
14	Tomblaine	1959-2005
15	Augny	1959-2005
16	Boulogne sur mer	1955-2005
17	Epinoy	1955-2005
18	Strasbourg	1959-2005
19	Mont Saint Vincent	1953-2005
20	Sainte Adresse	1955-2005
21	Vélizy Villacoublais	1954-2005
22	Saint Georges la Baulche	1954-2005

501 Table 1: list of the observed time series locations with their observation period considered for  
502 present climate  
503

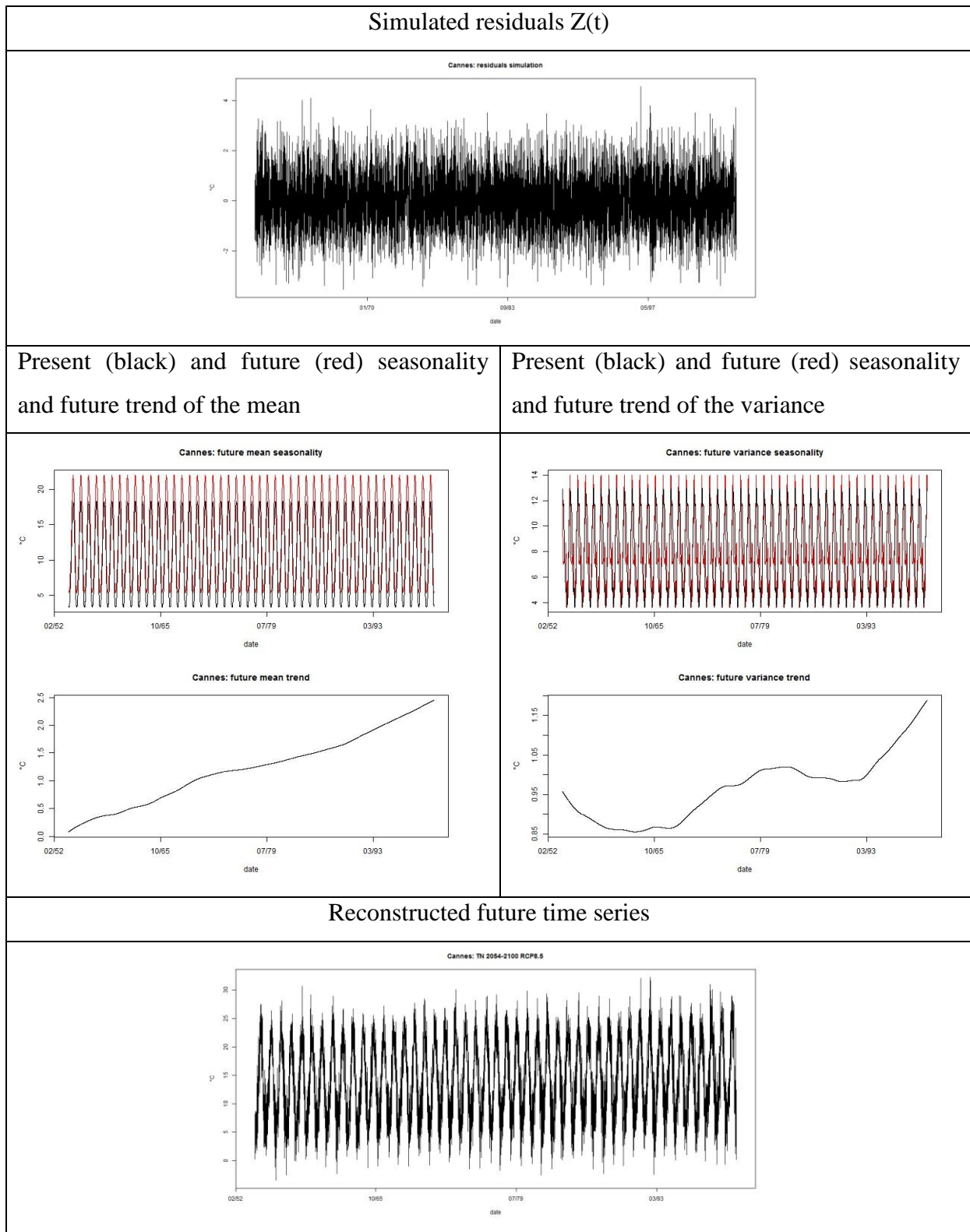


505  
506  
507  
508

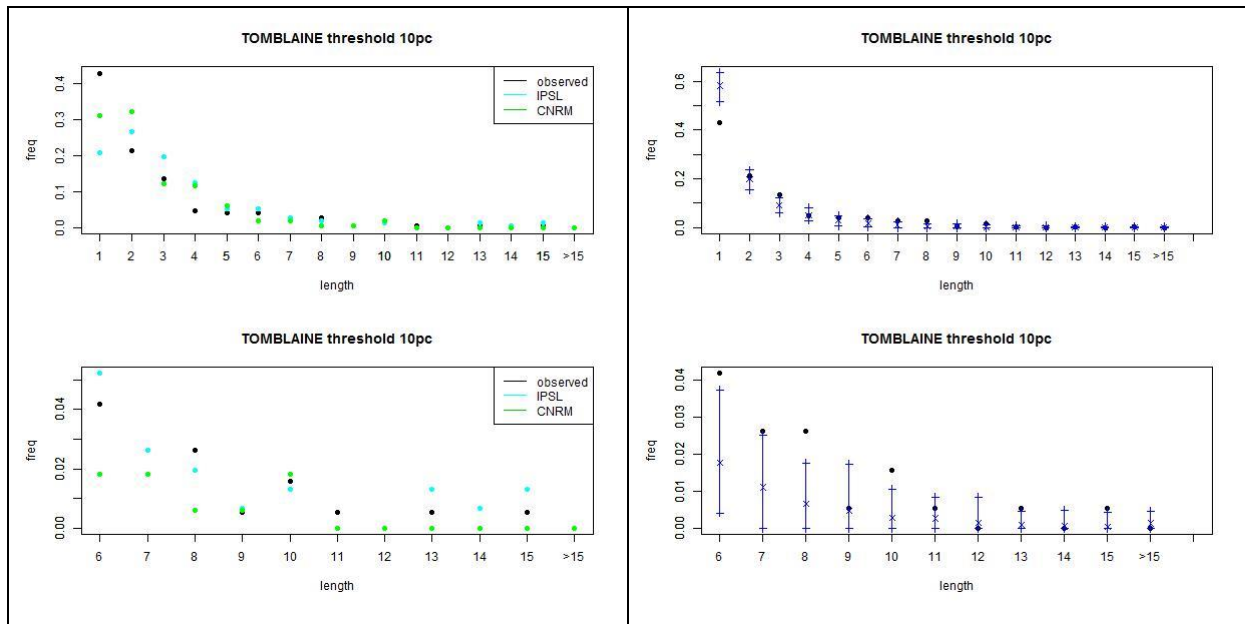
Figure 1: location of the 22 selected daily minimum temperature time series; the numbers refer to table 1 for the location identification



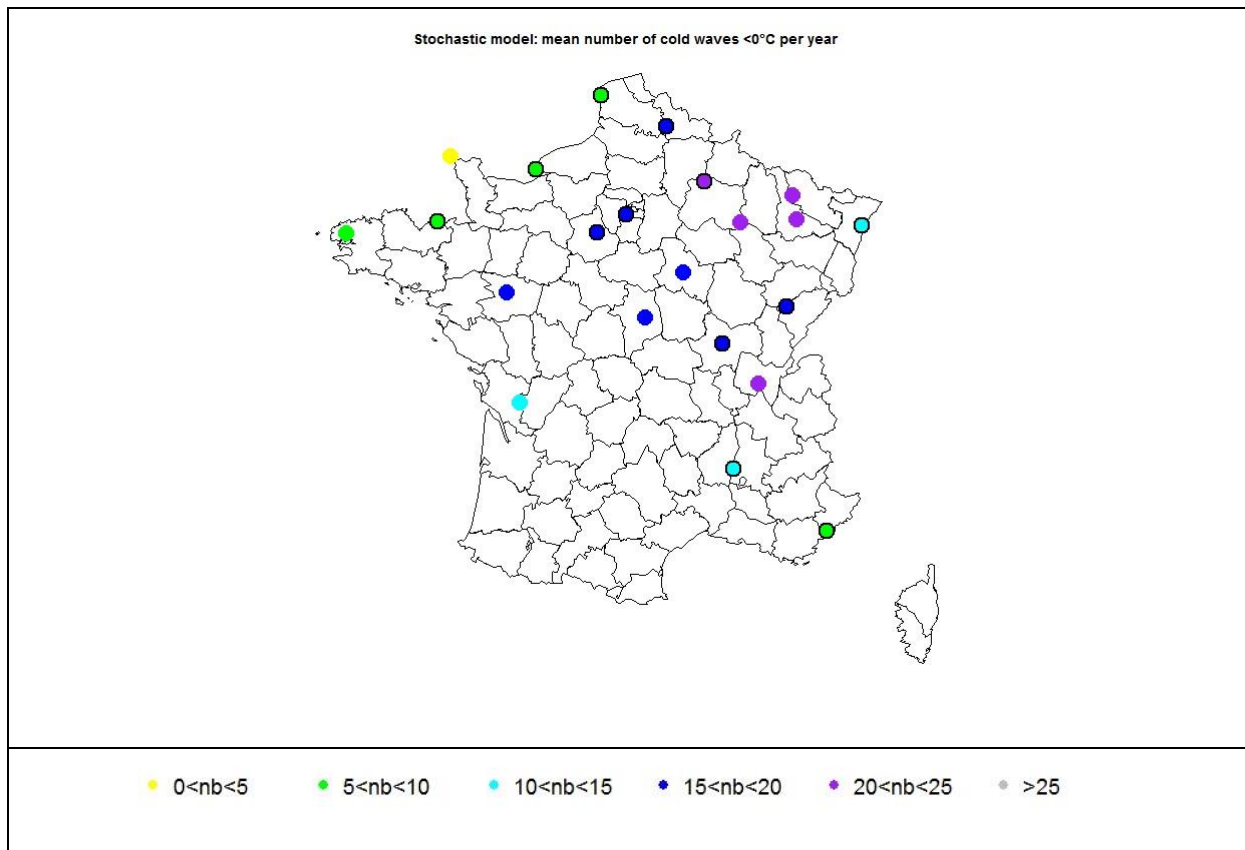
510 Figure 2: seasonality (top panel: mean top and variance bottom) and trend (bottom panel:  
 511 mean top and variance bottom) of the observed (black curves), IPSL-CM5A-MR (cyan) and  
 512 CNRM-CM5 (green) daily minimum temperature time series for Cannes, in the south of  
 513 France  
 514



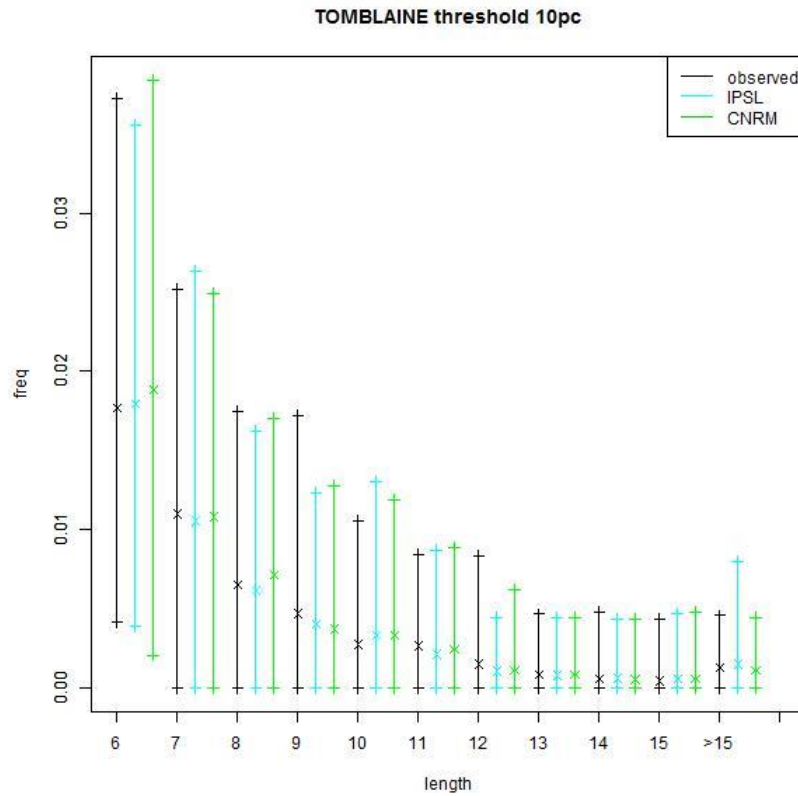
516 Figure 3: reconstruction of a future daily minimum temperature time series (bottom panel)  
 517 from the simulated residuals (top panel), the future seasonalities and trends (middle panel, for  
 518 seasonality: black = present, red = future) for the mean (left panel) and the variance (right  
 519 panel)



520 Figure 4: cold spells repartition with a 10<sup>th</sup> percentile threshold from the climate models (left  
 521 panel: observation in black, IPSL-CM5A-MR in cyan and CNRM-CM5 in green) and with  
 522 the stochastic model (right panel: observation in black, distribution for the 100 simulations in  
 523 blue: x mean and + 2.5 and 97.5 percentiles) for the station of Tomblaine. Top plots represent  
 524 all cold wave lengths while bottom plots zoom on the longest ones (6 days and more)  
 525

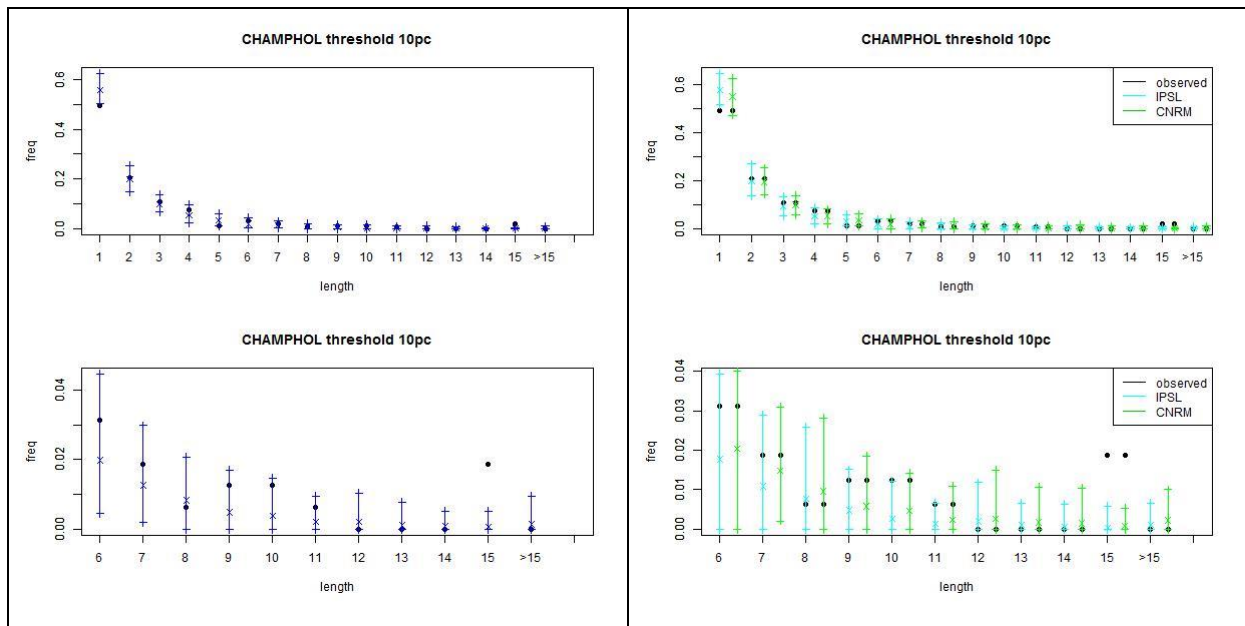


527 Figure 5: mean number of observed cold spells per year with 0°C threshold. Black circling  
 528 denotes the locations where the observed number does not fall inside the 95% confidence  
 529 interval of the stochastic simulations



531  
 532 Figure 6: distributions of proportions of the longest cold waves (6 days and more) obtained  
 533 with the stochastic model for the station of Tomblaine from the observations (simulated  
 534 residuals + observed seasonalities and trends, black), and from IPSL-CM5A-MR (blue) and  
 535 CNRM-CM5 (green) (simulated residuals + observed seasonalities and model trends). Cross  
 536 is for the mean value, and start and end of the segments are the 2.5 and 97.5 percentiles of the  
 537 distribution obtained from the 100 simulations

538  
 539  
 540  
 541  
 542  
 543  
 544  
 545  
 546  
 547  
 548  
 549

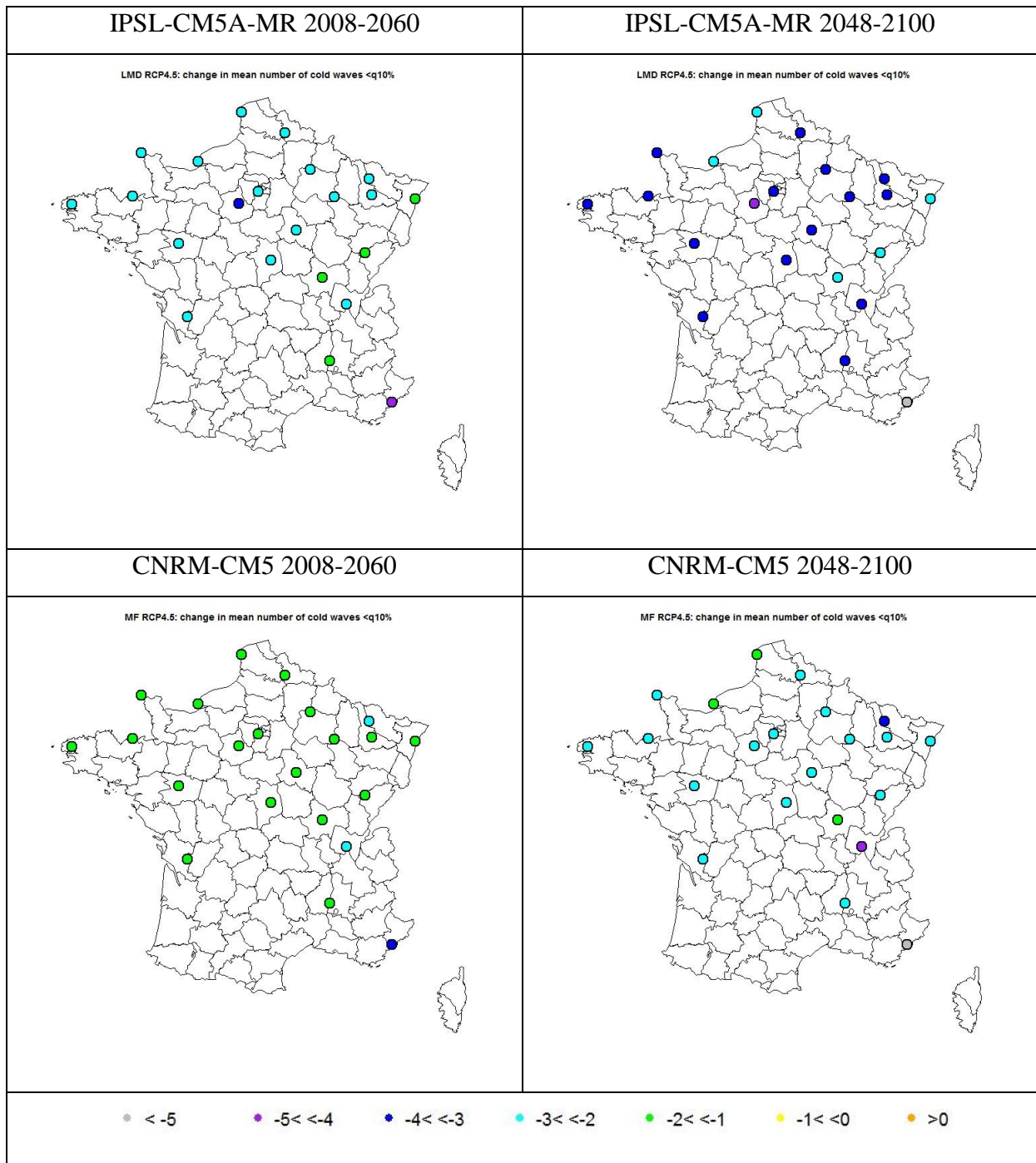


551 Figure 7: cold waves repartition with a 10<sup>th</sup> percentile threshold for the station of Champhol  
 552 over period 1980-2005 as given by direct fitting of the stochastic model on the observations  
 553 (left panel) or by reconstruction using climate model trends and seasonality increments (right  
 554 panel, IPSL-CM5A-MR in cyan and CNRM-CM5 in green) and stochastic model fitted over  
 555 period 1954-1979. Black points are for observed proportions while each bar represents the  
 556 distribution of the 100 simulations (x for mean and + for 2.5 and 97.5 percentiles). Top plots  
 557 represent all cold wave lengths while bottom plots zoom on the longest ones (6 days and  
 558 more)

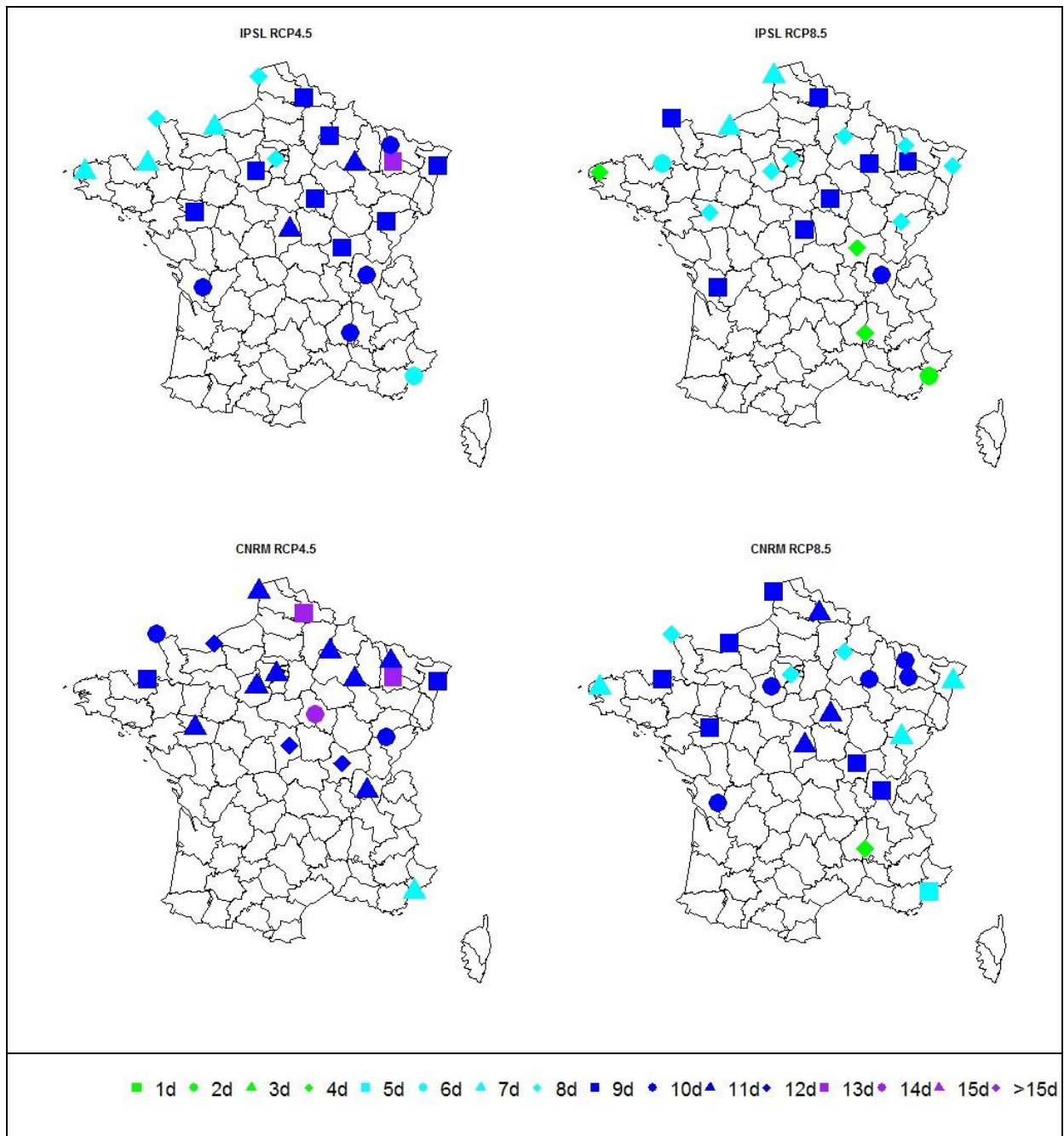
559

560

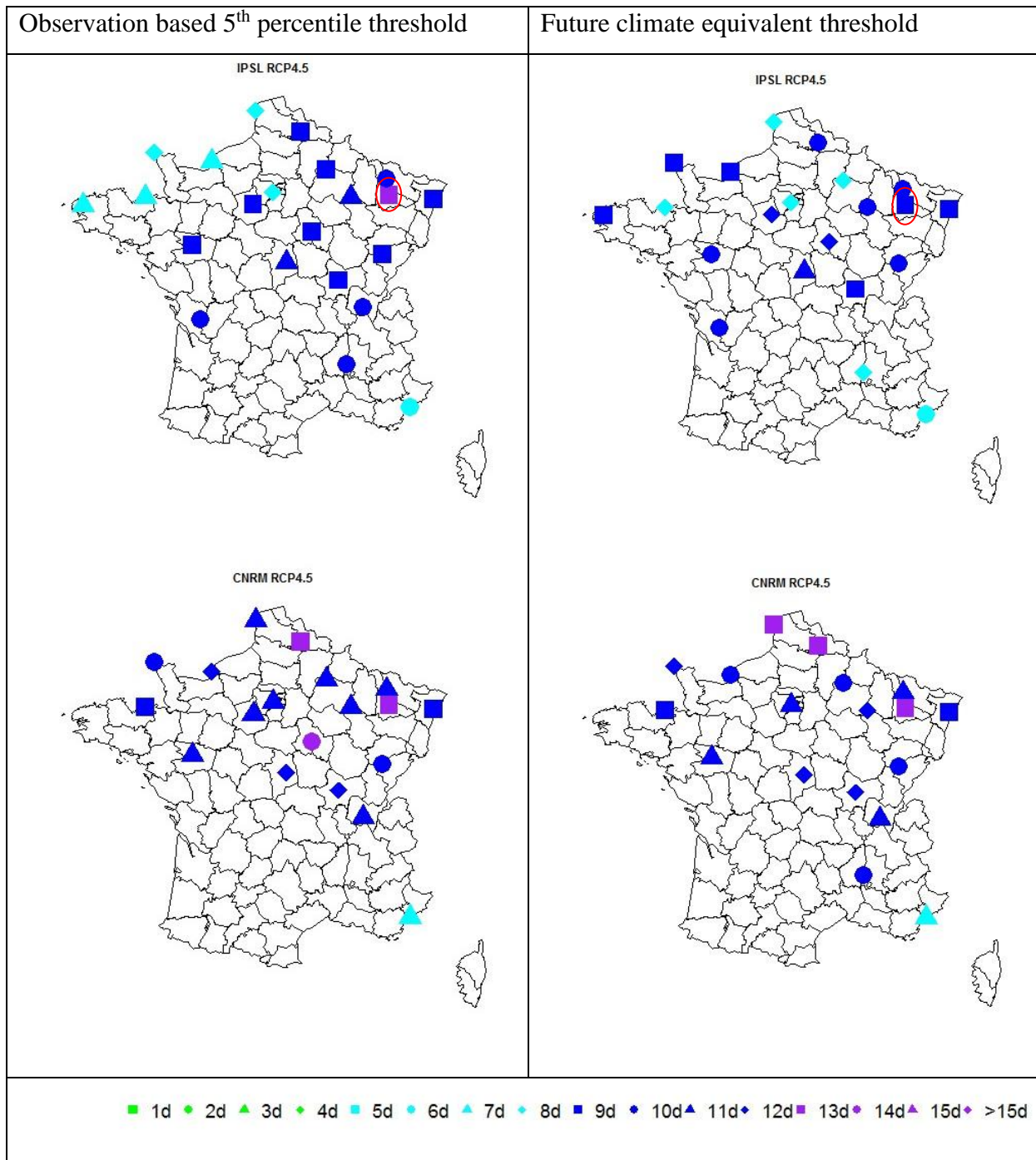




562 Figure 8: change in the mean annual number of cold waves of all duration for the near (ending  
563 in 2060, left panel) and far (ending in 2100, right panel) future periods with IPSL-CM5A-MR  
564 (top plots) and CNRM-CM5 (bottom plots) models with RCP4.5 with the 10<sup>th</sup> percentile  
565 threshold  
566



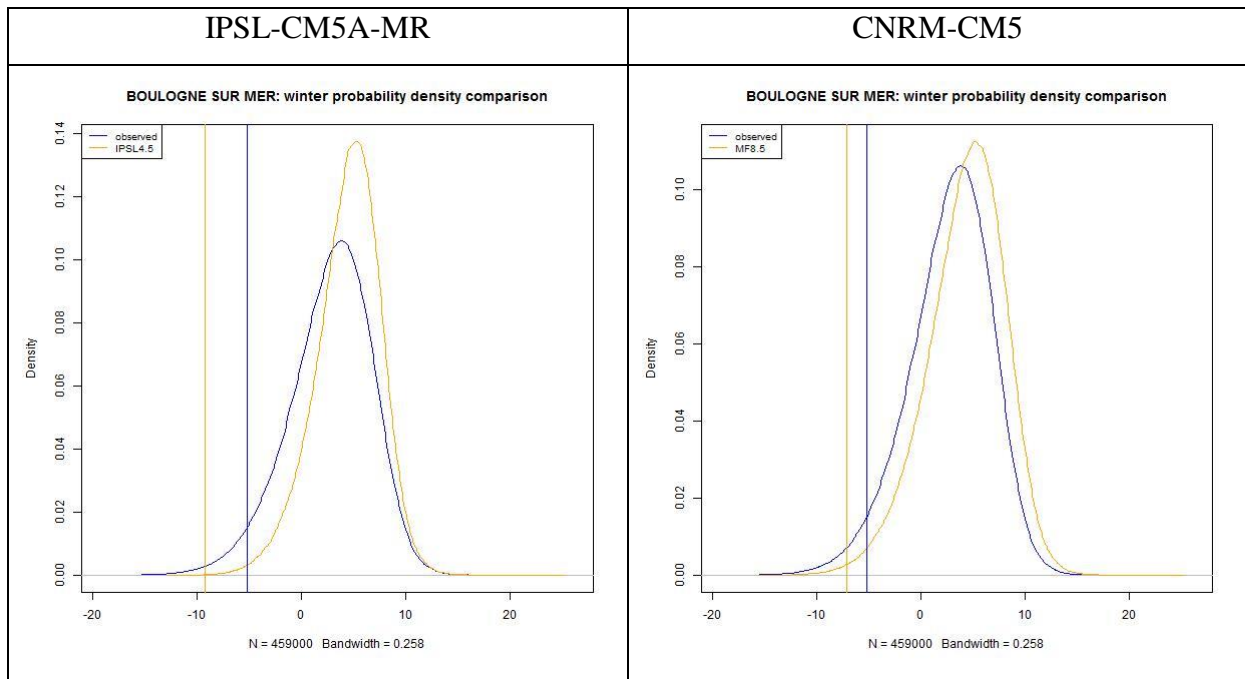
568 Figure 9: length from which the proportion significantly changes from the observed  
 569 proportion for future period ending in 2100 according to IPSL-CM5A-MR (top) and CNRM-  
 570 CM5 (bottom) models with RCP4.5 (left panels) and RCP8.5 (right panels) with the 5<sup>th</sup>  
 571 percentile threshold  
 572



574 Figure 10: length from which changes in proportions of cold waves are significant from the  
 575 observation based stochastic simulations with the observation based 5<sup>th</sup> percentile threshold  
 576 (left panel) and a threshold corresponding to the rank of this observation based 5<sup>th</sup> percentile  
 577 threshold in the far future (ending in 2100) wintertime temperature distribution (right panel).  
 578 Red circling isolates the station of Tomblaine which is further discussed

579

580



582 Figure 11: probability density function of the wintertime daily minimum temperature  
 583 according to the observations (blue curve) and climate model far future period with RCP4.5  
 584 (orange curve) with IPSL-CM5A-MR (left panel) and CNRM-CM5 (right panel). The blue  
 585 line is for the observation based 5<sup>th</sup> percentile threshold and the orange one for its equivalent  
 586 percentile in the future distribution